2010

Theoretical Detection Limits of Magnetic Biobarcode Sensors and the Phase Space of Nanobiosensing

Pradeep R. Nair
Purdue University - Main Campus, pnair@purdue.edu

Muhammad A. Alam
Purdue University - Main Campus, alam@purdue.edu

Nair, Pradeep R. and Alam, Muhammad A., "Theoretical Detection Limits of Magnetic Biobarcode Sensors and the Phase Space of Nanobiosensing" (2010). *Birck and NCN Publications.* Paper 747.
http://dx.doi.org/10.1039/C0AN00477D

Theoretical detection limits of magnetic biobarcode sensors and the phase space of nanobiosensing

Pradeep R. Nair* and Muhammad A. Alam*

Received 5th July 2010, Accepted 30th July 2010
DOI: 10.1039/c0an00477d

A scaling theory of the sub atto-molar (aM) detection limits of magnetic particle (MP) based biosensors (*e.g.*, bio-barcode assays) is developed and discussed. Despite the dramatic differences of sensing protocols and detection limits, the MP-based sensors can be interpreted within the same theoretical framework as any other classical biosensor (*e.g.*, nanowire sensors), except that these sensors are differentiated by the geometry of diffusion and the probe (ρ_{MP})/target (ρ_T) density ratio. Our model predicts two regimes for biomolecule detection: For classical biosensors with $\rho_{MP} \leq \rho_T$, the response time $t_s \propto 1/\rho_T$; while for MP-based biosensors with $\rho_{MP} > \rho_T$, $t_s \propto 1/\rho_{MP}$. The theory (i) explains the performance improvement of MP-sensors by ρ_{MP}/ρ_T (order of 10^3–10^6), broadly validating the sub-aM detection limits reported in literature, (ii) offers intuitive interpretation for the counter-intuitive ρ_T-independence of detection time in MP-sensors, (iii) shows that statistical fluctuations should reduce with ρ_T for MP sensors, and (iv) offers obvious routes to sensitivity improvement of classical sensors.

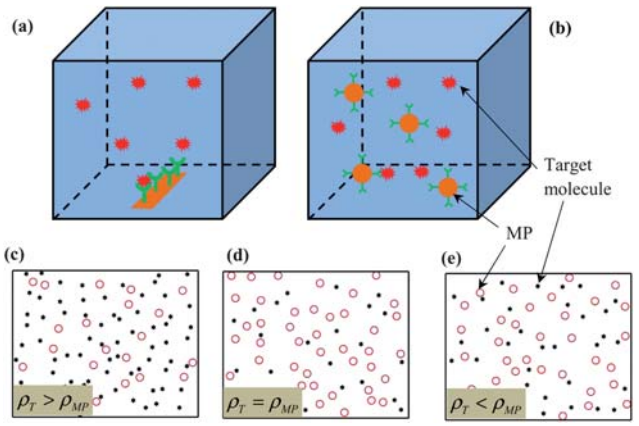

Fig. 1 (a) Classical biosensor with the sensor at rest and waiting for the molecules to arrive on the surface. (b) Magnetic particle sensor: magnetic particles functionalized with the capture probes are distributed in the system. (c)-(e) Schematics illustrating the different regimes of bio-molecule (solid dots) detection by MPs (open circles). (c) indicates $\rho_T > \rho_{MP}$, (d) $\rho_T = \rho_{MP}$, and (e) $\rho_T < \rho_{MP}$.

Introduction

Conventional biosensors consist of a single sensor element introduced into fluid volume containing many analyte or target biomolecules (Fig. 1a). Typically, the sensor is at rest and the target molecules diffuse to the sensor surface to produce a response. This geometry of target diffusion dictates the performance limits of modern nano-biosensors,[1–3] which is defined as the minimum detectable concentration for a given settling (or incubation) time. For example, analysis for nanowire (NW) sensors suggests the possibility of achieving ~ pico-molar (pM) detection limits, although the statistics of arrival time distribution could improve the detection limits to femto-Molar (fM) regime for an array of identically functionalized sensor elements.[4] Classical sensors, however, are presumed inadequate for sub-fM detection, and other schemes – particularly those involving magnetic particles (MP-sensors) – appear to extend the detection limits to sub-aM levels at reasonable settling times.[5–7] An enduring puzzle for the field is the underlying physics that dictates this remarkable detection limit of MP-sensors and whether other detection schemes could achieve comparable performance.

The practical protocol of MP based BioBarcode assays is very different from that of classical NW-based sensing. The method consists of four basic steps (see ref. 8 for detailed methodology): (A) target capture with receptor functionalized iron oxide MPs (see Fig. 1b), (B) subsequent incubation with Au nanoparticles (NP) functionalized with barcode molecules to form MP-target-NP conjugate, (C) magnetic field assisted localization of MP-target-NP conjugates, and (D) release and detection of barcode molecules. The barcode molecules are unique for each target species and enable multiplexed detection of biomolecules. The settling time for MP based sensors is dictated by the slowest of the above described four step process. Of them, Step A, the capture of target molecules at aM concentration with MPs (MP density, $\rho_{MP} \approx 0.1pM$), determines the eventual settling time. Step B is much faster than step A as the NPs are introduced at a much higher density ($1000 \times \rho_{MP}$). The time taken for the magnetic field assisted localization (step C) is of the order of few minutes as the terminal velocity[9] of MP conjugates (radius $a_0 = 0.5\mu m$, typical external field of B = 16mT) is of the order $10^2\mu m/s$. As Step C results in a concentration amplification, the detection time of the barcode molecules (Step D) can be reduced significantly. Hence the performance limits of MP based sensors are dictated by step A, the dynamics of target molecule capture by MPs. As mentioned before, if MP-sensors allow faster detection for a given analyte concentration, the trade off can then be used to achieve higher sensitivity for a given detection time.

The apparent complexity of biobarcode sensors has so far precluded theoretical interpretation for its detection limits and has made it difficult to explore prospects for performance enhancement. Indeed, classical Monte-Carlo study of MP sensors that would allow millions of magnetic particles and bio-molecules to diffuse randomly until conjugation is a computationally challenging task and has never

School of Electrical and Computer Engineering, Purdue University, West Lafayette, IN, USA. E-mail: pnair@purdue.edu; alam@purdue.edu

been attempted. In this Letter, instead, we use a novel reformulation of the problem to establish the theoretical limits of biomolecule detection by classical (Fig. 1a) and MP-sensors (Fig. 1b) through a combination of analytic and numerical methods. The detailed derivation will be discussed below, however, here is the key result that is broadly consistent with the available experimental data reported in the literature: For a system with ρ_T being the target molecule density and ρ_{MP} magnetic particle density, the settling time, defined as the average time to capture the target molecules, is given as

$$t_s = \frac{N_s}{4\pi\rho_T D a_0} \qquad (\rho_{MP} \leq \rho_T, N_s \geq 1), \tag{1a}$$

$$t_s = \frac{N_s}{4\pi\rho_{MP} D a_0} \qquad (\rho_{MP} \geq \rho_T, N_s = 1) \tag{1b}$$

where a_0 is the radius of the magnetic particle, D the diffusion coefficient, and N_s is the number of target molecules to be captured per magnetic particle for detection. Note that the settling time of classical NW sensors is also given by Eqn (1a), where a_0 is the radius of NWs. Eqn (1) predicts that MP sensors out-perform classical sensors by a factor ρ_{MP}/ρ_T. Let us now begin with an analytical derivation of eqn (1) and then discuss the profound implication of this result for nanoscale biosensors.

Model system

As described in Introduction, Step A determines the performance limits of MP based sensors. To study the dynamics of target molecule capture by MPs, let us now consider a MP-sensor in which target biomolecules and MPs are uniformly distributed (Fig. 1b, also see Fig. 1(c)–(e) for an illustration in 2D) over the fluidic volume. The target molecules execute random walks and are eventually captured by the MPs (isotropically functionalized by capture probes) if they wander close to the receptors. As we focus on the theoretical detection limits, we assume negligible MP-MP or MP-target interferences during target capture, because for a typical MP density of 0.1pM (equivalent to 0.25mg/mL, ref. 7), the MPs are many tens of microns apart. As the MPs are paramagnetic, they do not interact among themselves during the capture phase when magnetic fields are absent. And, while both MPs as well as the targets are mobile, the larger dimensions of MPs make their thermal diffusion negligible (MP diameter $\sim 1\mu m$, while the molecule size is of the order of few nm). Therefore, for all practical purposes, the absolute lower limits for capture, or settling time, is only dictated by the diffusion of target molecules towards the quasi-stationary background of MPs given by:

$$\frac{\partial \rho}{\partial t} = D\nabla^2\rho \tag{2a}$$

where D is the effective diffusion coefficient of target molecules and ρ is the density of target molecules ($\rho = \rho_T$, at $t = 0$). To determine the detection limits, we assume that the MP surface is characterized by the idealized boundary condition,

$$\rho = 0 \tag{2b}$$

i.e., the capture is irreversible *i.e.*, the targets are captured the very first time it interacts with the MP, and the number of targets captured is much smaller than the number of receptors available per MP. In practice, finite capture probability will only degrade the limit. Since the particle flux at the MP surface is given by $J(t) = D\nabla_n\rho$, ρ being the solution of eqn (2), the number of molecules captured on the nanoparticle surface, N(t), is then given by

$$N(t) = 4\pi a_0^2 \int_0^t J(t)dt, \tag{3}$$

where a_0 is the radius of MP. Eqn (3) assumes isotropic diffusion of target molecules towards MP and is valid even in the dilute limit as an ensemble average of individual capture processes. We now consider two regimes of bio-molecule detection based on the relative density of target molecules and magnetic particles.

Case 1 ($\rho_T \geq \rho_{MP}$)

Here the magnetic particles are sparsely distributed in volume containing target molecules (Fig. 1c) – similar to the situation of classical NW-sensors (Fig. 1a). The diffusive flux towards a perfectly adsorbing MP (from ref. 2,10, analytic solution for eqn (2)) is given by $J(t) = \frac{D\rho_T}{a_0}(1 + \frac{a_0}{\sqrt{6Dt}})$. Using eqn (3), we obtain $N(t) = 4\pi\rho_T D a_0 \left(t + (a_0/\sqrt{6D})t^{1/2}\right)$. Retaining only the leading terms (since $a_0/\sqrt{6D} \ll 1$), the settling time, t_s, required to capture a certain threshold, N_s, of the target molecules is given by $t_s = N_s/4\pi\rho_T D a_0$, the first relation of eqn (1). Since $\rho_T > \rho_{MP}$, each MP can capture multiple particles and the parameter N_s is determined by the sensitivity of the detection scheme.

In the limiting case of $\rho_T = \rho_{MP}$, the MP and target molecules have the same density (Fig. 1d). As the MPs are presumed not to interact with each other in terms of molecule capture, the kinetics of capture is still defined by eqn 1 (a), until the statistically averaged number of target molecules captured (N_s) by each nanoparticle becomes unity. At that time, all the molecules are captured by the MPs (since $\rho_T = \rho_{MP}$) and the system reaches steady state. Hence the settling time for this case is also given by $t_s = N_s/4\pi\rho_T D a_0$, with $N_s = 1$.

Case 2 ($\rho_T \leq \rho_{MP}$)

In the other extreme case typical of MP-sensors (Fig. 1b), the MPs outnumber the targets biomolecules by several orders of magnitude. Assuming a background of quasi-stationary MPs, the diffusion of target molecules is described by integrating eqn (2a) and eqn (2b) into a single equation, as follows:

$$\frac{\partial \rho}{\partial t} = D\nabla^2\rho - \alpha\rho_{MP}\rho. \tag{4}$$

Here, the second term on the RHS denotes the rate of capture of the target molecules by the MPs. The constant α can be evaluated as follows: Recall that the flux towards a MP is given by $J(t) \approx D\rho_T/a_0$ (see previous section on Case 1, $\rho_T \geq \rho_{MP}$). Hence the net rate of conjugation of target molecules with MPs, $F(t)$, is given by $F(t) = \rho_{MP}(4\pi a_0^2)J(t) = 4\pi a_0 D\rho_{MP}\rho_T$. Comparing with the second term on the RHS of eqn (4), we obtain $\alpha = 4\pi a_0 D$.

Assuming that a single target molecule is released at time $t = 0$ at $r = 0$ (*i.e.*, the excitation is delta function in both time and space), the solution for eqn (4) is given as

$$\rho(r,t) = At^{-3/2}e^{-t/\tau}e^{-\left(\frac{r^2}{4Dt}\right)} \quad (5)$$

where A is constant (such that solution represents a delta function in space and time at $r = 0$, $t = 0$) and $\tau \equiv 1/\alpha\rho_{MP}$. The survival probability, S(t), of the particle is given as

$$S(t) = \frac{\int_0^\infty \rho(r,t)4\pi r^2 dr}{\int_0^\infty \rho(r,t=0)4\pi r^2 dr} = \frac{e^{-t/\tau}}{\tau}. \quad (6)$$

Hence the average settling time is τ and is given as

$$t_s = \tau = \frac{1}{4\pi\rho_{MP}Da_0}. \quad (7)$$

Remarkably, for $\rho_T < \rho_{MP}$, the settling time is independent of the density of the target molecule ρ_T, as all capture events are independent of each other and depends only on MP density ρ_{MP} (see Fig. 1e). This completes the derivation of eqn 1(b), *i.e.* $t_s = N_s/4\pi\rho_{MP}Da_0$, with $N_s = 1$.

Numerical validation

To validate the analytical solution, we solve eqn (2) both numerically by finite element (FE) as well as Monte Carlo (MC) methods. In MC simulations, the many particle random walk is simplified by assuming an ensemble of two-particle diffusive system that gives, as an ensemble average, the same results as the many particle system. In this two-particle MC formulation, the MP is assumed to be static and the target molecules are allowed to perform random walk in 3 dimensions. For $\rho_T = \rho_{MP}$, the simulation volume is given as $V_{box} = \rho_T^{-1}$ while for $\rho_T < \rho_{MP}$, V_{box} is determined by the minimum of (ρ_T^{-1}, ρ_{MP}^{-1}). The system is simulated with periodic boundary conditions and the target is assumed to be captured by the MP upon first contact. The parametric dependence of capture time (t_s) on various configurations of target-MP separation is first estimated and the statistical average over a large number (10^5) of pair-configurations is used to estimate the mean capture time. Numerical results shown in Fig. 2 indicate that MC simulations successfully reproduce the analytical results. Note that for $\rho_T \leq \rho_{MP}$, the settling time is independent of ρ_T, a surprising result and can be explained as follows: For $\rho_T \leq \rho_{MP}$ (see Fig. 1e), the average capture time is dictated by the mean diffusion distance of target molecules to an available MP, which is exclusively determined by the MP density and is independent of ρ_T. *Hence, the average capture time or settling time is independent of* ρ_T, *however, the net number of captured molecules scale with* ρ_T, *as expected.* This key result is supported by direct experimental evidence from ref. 6. Specifically, ref. 6 shows that the fluorescence spot intensity increases with DNA target density, while the assay time is independent of DNA target density, supporting our simulation results.

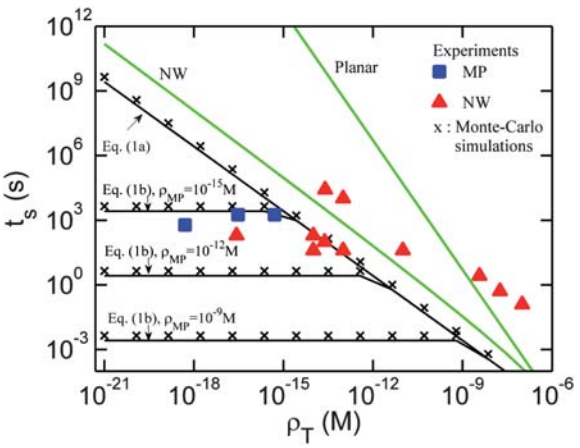

Fig. 2 Settling time as a function of target molecule density ($N_s = 1$). Analytic solutions are shown as solid lines while Monte-Carlo simulation results are shown as 'x' symbols. The settling time for NW (radius 50nm, length- 1μm, time to capture $N_s = 3$ molecules per NW) and planar sensors, based on ref. 2, are also plotted. The simulation parameters are: $D = 10^{-6}cm^{-2}/s$, $a_0 = 0.5\mu m$.The solid squares represent experimental data using MP sensors (ref. 5–7) while the solid triangles represent experimental data using NW sensors from various groups (ref. 14–19). The theoretical results on the performance limits of planar, NW, and MP sensors can also be accessed through an online simulation tool, *BioSensorLab*.[20]

Implications

Eqn (1) and Fig. 2 provide a phase diagram for sensor response for planar, cylindrical, and MP sensors and show how a single unifying framework interprets the detection limits of each technology. It is obvious from the plot that the settling time of a sensor can be reduced by a factor of ρ_{MP}/ρ_T for the case where sensors outnumber target molecules. Indeed, practical MP detection schemes like biobarcode assays[6] report $\rho_{MP}/\rho_T \sim 10^3 - 10^6$, which not only reduces the detection time dramatically, but also offers the possibility of sub-aM detection within reasonable detection times, as opposed to days of incubation time required for classical sensors.[1–3] Note that MP-sensors beat the classical diffusion limit associated with cylindrical or planar sensors by a 'divide-and-search' strategy, so that no single sensor need to search beyond a very short diffusion-limited regime. As we assumed infinite conjugation rates between the target molecules and receptors attached to the MP (as indicated by eqn (2b)), eqn (1) indeed predict the absolute lower limits of detection time and hence the performance limits of the technology.

The methodology based on MP-based detection significantly reduces the statistical distribution of the capture time compared to classical biosensors. Following eqn (6), for $\rho_T \leq \rho_{MP}$, the density of target molecules that survive after time t is $\rho_{surv} = \rho_T e^{-t/\tau}$. We define the maximum waiting time (t_{max}) as the time taken to capture the last surviving molecule. At $t = t_{max}$, we have $\rho_T e^{-t_{max}/\tau} \approx 1/V_{sample}$, where V_{sample} is the sample volume under consideration. Correspondingly, we find that

$$t_{max} \propto \frac{\log(V_{sample}\rho_T)}{\rho_{MP}} \quad (8)$$

i.e., the maximum waiting time reduces with ρ_T ($V_{sample}\rho_T$ is the total number of target molecules present in the sample). This surprising result can be intuitively explained as follows: For $\rho_T \leq \rho_{MP}$, larger the number of target molecules in the system, larger would be the time taken for all of them to be captured. Hence t_{max} is expected to be proportional to $\log(\rho_T)$. In contrast to classical sensors where randomness in arrival time of molecules to the sensor surface increases with decrease in ρ_T (ref. 4), for MP sensors, the maximum waiting time or rather the randomness in the settling time distribution

decreases with dilution of target molecules (a conclusion supported by MC simulations). Eqn (8) also indicates that the fluctuations in the settling time can be reduced by increasing ρ_{MP}, an intuitive result.

Finally, the 'Selectivity' MP-sensors – defined as the ability of a sensor to avoid 'false-positive' during the parallel detection of many biomolecules – is considerably improved because unlike classical electronic sensors, the magnetic field is not contaminated by electrostatic screening due to ions in the solution.[11] Moreover, being a labeled scheme (magnetic particles act as labels), these schemes are not affected by physisorbtion of parasitic molecules on the sensor surface and the associated background noise.[12]

Can classical label-free sensors be redesigned to achieve detection limits comparable to MP-sensors? Recall that the fast response of MP-sensors arises from the condition that $\rho_T \ll \rho_{MP}$ and $N_s = 1$, so that the maximum diffusion distance for the target molecules scales inversely as the density of MPs. Classical sensors (*e.g.*, Silicon NW) on the other hand operates at the opposite limit of $\rho_T \gg \rho_{MP}$ and $N_s > 1$, where the target molecule far outnumber the sensor elements and the diffusion-limit dictates that the settling-time scale inversely with target density.[2] Instead, if NW-sensors could adopt a scheme analogous to MP-sensors (*i.e.*, $\rho_T \ll \rho_{MP}$ and $N_s = 1$) by distributing the total analyte volume in a individually accessible (but physically partitioned) parallel array of micro-wells, each decorated with identically labeled NW-sensors with *single molecule detection capability*, the fragmentation of space would allow the label-free sensors approach the detection limits of MP-sensors. Single molecule detection capability ($N_s = 1$) is crucial as the probability of finding $N_s > 1$ molecules in a micro-well reduces exponentially (the target molecules at extreme low concentrations follow Poisson distribution, similar to the formation of defects in an oxide dielectric[13]). However, this can be addressed through appropriate signal amplification schemes for single molecule detection capability and the advances in lithography and interconnects makes such parallelization of label-free detection scheme feasible.

Practical considerations: In this article we developed the *theoretical* detection limits of a promising technology using magnetic particles – for which no simple first order estimate is available in literature. With the theoretical detection limits being the focus, we idealized each step so as to establish maximum limit of detection (*e.g.*, infinite rate of conjugation between the target and MP, negligible MP-MP interactions, background noise, *etc.*). Our assumption of infinite conjugation rate does not suggest that chemical reactions are unimportant, instead suggest that even if we could design a chemical reaction that is fast enough not to be a bottleneck of the system performance, still there is a theoretical limit of detection associated with two set of particles (MP and the target) 'looking for' each other in a solution. Similarly MP size and surface functionalization are important design aspects to prevent agglomeration and MP-MP interactions. These limitations would certainly influence the performance and reduce the sensitivity and could be interesting topics for future research. However, the absolute lower limits of sensitivity (in a statistically averaged sense) are still predicted by eqn (1) of this article.

Conclusions

In summary, we have provided the first scaling theory for the sub-aM detection limits of magnetic particle based biosensors and connects it – possibly for the first time – with the detection limits of classical planar or nanowire sensors. Our model explains the orders of magnitude performance improvement of MP-sensors, broadly validating the sub-aM detection limits reported in literature and offers intuitive interpretation for the counter-intuitive ρ_T-independence of detection time in MP-sensors. We show that statistical fluctuations should reduce with ρ_T for MP sensors and our results offer obvious routes of optimization for classical sensors.

Acknowledgements

The authors acknowledge computational and financial support from Network of Computational Nanotechnology (NCN), National Institute of Health (NIH-R01CA120003), and Materials Structures and Devices Center of the Semiconductor Research Center - Focus Center Research Program (MSD 104309).

References

1 P. E. Sheehan and L. J. Whitman, Detection limits for nanoscale biosensors, *Nano Lett.*, 2005, **5**(4), 803–807.
2 P. R. Nair and M. A. Alam, Performance limits of nanobiosensors, *Appl. Phys. Lett.*, 2006, **88**(23), 233120.
3 T. M. Squires, R. J. Messinger and S. R. Manalis, Making it stick: convection, reaction and diffusion in surface-based biosensors, *Nat. Biotechnol.*, 2008, **26**(4), 417–426.
4 J. Go and M. Alam, Statistical interpretation of "femtomolar" detection, *Appl. Phys. Lett.*, 2009, **95**(3), 033110.
5 E. Goluch, J. Nam and D. Georganopoulou, *et al.*, A bio-barcode assay for on-chip attomolar-sensitivity protein detection, *Lab Chip*, 2006, **6**(10), 1293–1299.
6 J. Nam, S. Stoeva and C. Mirkin, Bio-bar-code-based DNA detection with PCR-like sensitivity, *J. Am. Chem. Soc.*, 2004, **126**(19), 5932–5933.
7 J. M. Nam, C. S. Thaxton and C. A. Mirkin, Nanoparticle-based bio-bar codes for the ultrasensitive detection of proteins, *Science*, 2003, **301**(5641), 1884–1886.
8 H. D. Hill and C. A. Mirkin, The bio-barcode assay for the detection of protein and nucleic acid targets using DTT-induced ligand exchange, *Nat. Protoc.*, 2006, **1**, 324–336.
9 N. Pekas, M. Granger and M. Tondra, *et al.*, Magnetic particle diverter in an integrated microfluidic format, *J. Magn. Magn. Mater.*, 2005, **293**(1), 584–588.
10 S. Chandrasekhar, Stochastic problems in physics and astronomy, *Rev. Mod. Phys.*, 1943, **15**(1), 0001–0089.
11 P. R. Nair and M. A. Alam, Screening Limited Response of Nanobiosensors, *Nano Letters*, 2008, **8**(5), 1281–1285.
12 P. R. Nair and M. A. Alam, Theory of 'Selectivity' of Nanobiosensors: A Geometro-Physical Perspective, *J. Appl. Phys.*, 2010, **107**, 064701.
13 M. A. Alam, R. K. Smith and B. E. Weir, *et al.*, Thindielectric films - Uncorrelated breakdown of integrated circuits, *Nature*, 2002, **420**(6914), 378–378.
14 J. Hahm and C. M. Lieber, Direct ultrasensitive electrical detection of DNA and DNA sequence variations using nanowire nanosensors, *Nano Lett.*, 2004, **4**(1), 51–54.
15 G. F. Zheng, F. Patolsky and Y. Cui, *et al.*, Multiplexed electrical detection of cancer markers with nanowire sensor arrays, *Nat. Biotechnol.*, 2005, **23**(10), 1294–1301.
16 Z. Q. Gao, A. Agarwal and A. D. Trigg, *et al.*, Silicon nanowire arrays for label-free detection of DNA, *Anal. Chem.*, 2007, **79**(9), 3291–3297.
17 E. Stern, J. F. Klemic and D. A. Routenberg, *et al.*, Label-free immunodetection with CMOS-compatible semiconducting nanowires, *Nature*, 2007, **445**(7127), 519–522.
18 A. Kim, C. S. Ah and H. Y. Yu, *et al.*, Ultrasensitive, label-free, and real-time immunodetection using silicon field-effect transistors, *Appl. Phys. Lett.*, 2007, **91**, 103901.
19 W. Kusnezow, Y. V. Syagailo and S. Ruffer, *et al.*, Kinetics of antigen binding to antibody microspots: Strong limitation by mass transport to the surface, *Proteomics*, 2006, **6**(3), 794–803.
20 P. R. Nair and M. A. Alam, *BioSensorLab*, http://nanohub.org/resources/2929.